Tunability of a 2*e* periodic single Cooper pair box

David Gunnarsson,* Tim Duty, Kevin Bladh, and Per Delsing
Microtechnology and Nanoscience, Chalmers University of Technology, S-412 96, Göteborg, Sweden
(Received 23 July 2004; revised manuscript received 4 October 2004; published 30 December 2004)

We have measured the fully 2*e* periodic Coulomb staircase of a single Cooper pair box (SCB) in superconducting quantum interference design geometry, using a radio-frequency single-electron transistor. We have determined the energies of the SCB with microwave spectroscopy and compared the calculated shape of the Coulomb staircases to the measured staircases. We find excellent agreement as the Josephson coupling energy is tuned by an external magnetic field.

DOI: 10.1103/PhysRevB.70.224523 PACS number(s): 74.50.+r, 73.23.Hk, 85.25.Cp

I. INTRODUCTION

Study of mesoscopic solid state circuits in the quantum regime have gained a lot of interest lately, mainly due to the possibility of constructing two-level quantum systems as quantum bits (qubits), in a scalable quantum computer. Quantum circuits that use the quantum properties of Josephson junctions, where charge Q and phase ϕ are conjugated quantum variables, have been studied intensively.[1–7] Josephson circuits have the advantage that both the quantum system and the detector can be fabricated in the same technology and that the technology is in principle easily scalable. Reports of coherent quantum oscillations in Josephson circuits have recently been presented from a number of groups.[1–7]

However, to use a system as a qubit a good control over the energy levels is needed. In this paper we address the issue of controllability of one possible qubit system, namely, the single Cooper pair box (SCB).[8–11] We demonstrate controllability of both the charging energy and the Josephson coupling energy and demonstrate how the quantum smearing of the Coulomb staircase[12,13] is controlled by an external magnetic field.

II. THE SCB

The SCB consists of a superconducting island (box) connected to a reservoir through an ultrasmall Josephson junction. The SCB is characterized by its charging energy $E_C = e^2/2C_\Sigma$ and its Josephson coupling energy E_J, where e is the electron charge and C_Σ is the total capacitance of the island. The island's charge states are quantized into the number of excess Cooper pairs on the island. By controlling the electrostatic potential of the island, the charge state can be increased or decreased in steps of one Cooper pair.

The Hamiltonian of the SCB can be expressed in the charge basis $|n\rangle$, i.e., the number of excess Cooper pairs on the island. With a voltage V_g applied to a gate, which is capacitively coupled to the box, the effective number of induced Cooper pairs on the box, $n_g = C_g V_g/2e$, can be controlled. Here C_g is the capacitance between the gate and the box. Tunneling of Cooper pairs through the Josephson junction couples the different charge states with the associated Josephson coupling energy. Thus the Hamiltonian in the charge basis becomes

$$H = 4E_C \sum (n - n_g)^2 |n\rangle\langle n| - \frac{E_J}{2} \sum (|n+1\rangle\langle n| + |n\rangle\langle n+1|). \quad (1)$$

The curves of electrostatic energy versus induced charge n_g form a set of parabolas [dotted line in Fig. 1(a)] centered around $n_g = n = \ldots 0, 1, 2\ldots$, and at the parabola crossings the charge state changes by one Cooper pair. The charge state degeneracies at $n_g = n + \frac{1}{2}$ are lifted by the Josephson coupling energy and gaps open at degeneracy points [see Fig. 1(a)]. These energy bands are the same as for an isolated small junction.[14]

The charge of the ground state of the SCB thus increases in a steplike manner as the external voltage is increased, which results in the so called Coulomb staircase.[12,13] The tunneling due to E_J will smear the Coulomb staircase around the Cooper pair transition. The shape of the staircase thus depends strongly on E_C and E_J, so that the SCB's characteristic energies can be obtained from the shape, or vice versa. At finite temperatures T, the charge transitions will also be smeared due to thermal excitations, but here we will discuss only the behavior at low temperature.

There is also a possibility to add an extra quasiparticle to the box rather than an extra Cooper pair. The energy cost for this is the odd-even free energy difference $\tilde{\Delta} = \Delta(B) - k_B T \ln(N)$, where Δ is the superconducting gap and N is the effective number of states available for excitations.[15] If this energy is smaller than E_C the ground state for the box can be a quasiparticle state, with an odd number of electrons on the box. In this case the SCB loses its Cooper pair quantization and a 1*e* step will turn up in the Coulomb staircase [Fig. 1(b)].

The problem of getting a fully 2*e* periodic Coulomb staircase experimentally is a well known difficulty and has been discussed in several papers.[9,11,16–18] The reason for these problems is most probably the presence of nonequilibrium quasiparticles. Two ways to reduce this "quasiparticle poisoning" have been suggested and demonstrated. One way that has been successful is to add normal metal on the reservoir in close proximity to the SCB.[9] In the other method, which also has been shown successful, the superconductive gaps of leads and island are fabricated in such a way that $\Delta_{island} > \Delta_{leads}$.[17]

The state of the SCB can be detected with several different techniques. One way is to measure the current from re-

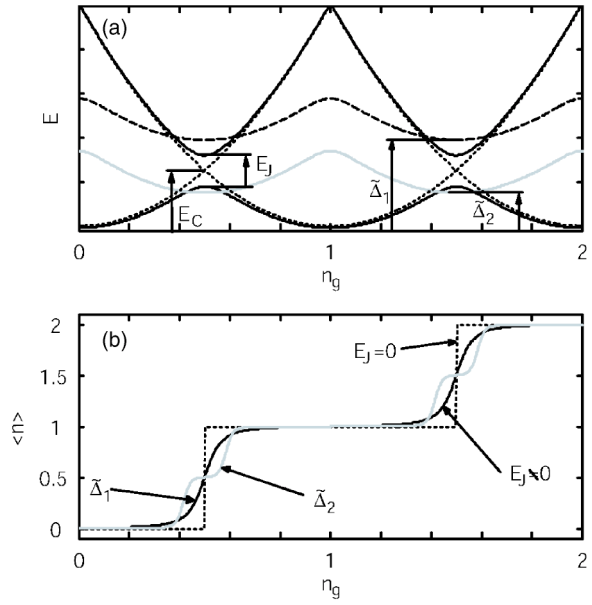

FIG. 1. (a) The energy for a SCB with $E_J=0$ (dotted) and $E_J \neq 0$ (solid). The dashed and gray lines indicate the odd charge state with $\tilde{\Delta}_1$ and $\tilde{\Delta}_2$, respectively. (b) The corresponding average charge $\langle n \rangle$ for the energy diagram in (a). The effect on the Coulomb staircase when the odd charge state is energetically favorable, $\tilde{\Delta}_2 < E_C - E_J/2$, is the appearance of the $1e$ step (gray solid line).

laxation of Cooper pairs by quasiparticle tunneling through a probe junction.[1] Alternatively one can measure the switching probability of a large Josephson junction integrated into the same circuit as the SCB,[2] or by measuring the charge of the box using an electrometer coupled capacitively to the box.[6,7,9,11,16]

A well suited electrometer that has subelectron sensitivity and can be fabricated with the same technology as the SCB is the single-electron transistor (SET).[19,20] We use a radio-frequency single-electron transistor[21] (rf SET) as an electrometer to determine the charge state of a SCB. The rf SET is an improvement of the SET that operates with increased bandwidth and sensitivity.[21,22]

The energies of the SCBs and their dependence on gate charge and magnetic field can also be extracted using spectroscopy.[16,23] Irradiating the SCB with microwaves of a frequency ν corresponding to the level splitting, the system can be brought to the excited state, which changes the charge of the box. By systematically measuring the charge of the box as a function of gate charge for several different microwave frequencies, E_C and E_J of the SCB can be extracted with very good accuracy [see Fig. 2(a)].

In this paper we discuss two samples which were measured under conditions such that they were $2e$ periodic. We describe measurements on the SCBs where we have done adiabatic measurements of the charge in the ground states. We have also performed spectroscopic measurements on the energy levels of the SCB. Using the data extracted from the spectroscopy we can calculate the ground state of the SCB and compare to the measured Coulomb staircases. We find an excellent agreement between the calculated and the measured staircases.

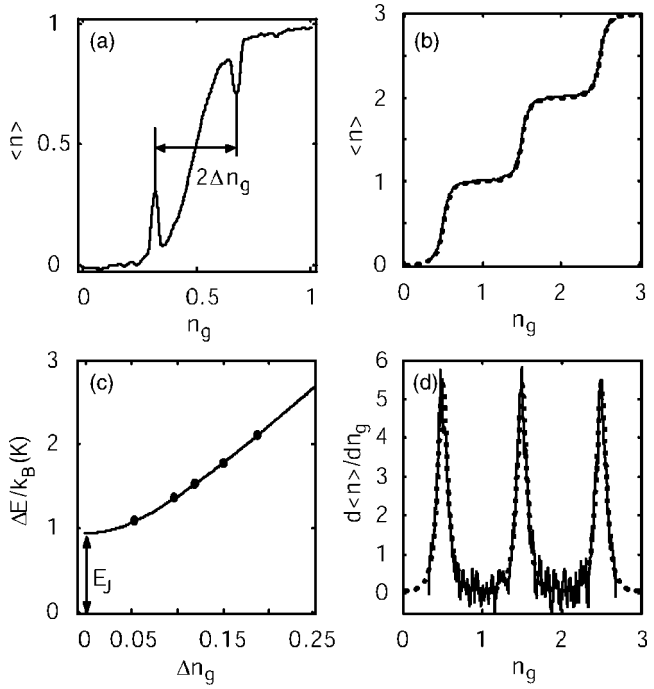

FIG. 2. (a) The Coulomb staircase when continuous microwaves are applied to the SCB for sample A. (b) The filled circles indicate the energy separation ΔE versus Δn_g for the applied frequencies $\nu_1=22.8$ GHz, $\nu_2=28.4$ GHz, $\nu_3=32$ GHz, $\nu_4=37.1$ GHz, and $\nu_5=44$ GHz. These points are fitted to ΔE with $E_C/k_B=1.25$ K and $E_J/k_B=0.94$ K (solid line). Data obtained from sample A. (c) The Coulomb staircase obtained at the same applied B as above (solid line) together with the calculated Coulomb staircase for $E_C/k_B=1.25$ K and $E_J/k_B=0.94$ K (dotted line). (d) Same as (c), but with the derivative of the Coulomb staircase.

III. EXPERIMENTAL DETAILS

Both the rf SET and the SCB are fabricated with electron beam lithography followed by two-angle shadow evaporation of aluminum on an oxidized silicon substrate. The SCB is fabricated in a superconducting quantum interference device (SQUID) geometry with two small Josephson junctions that connect the island to the reservoir. This gives us the possibility to tune the effective E_J by applying an external magnetic field.

The coupling between the rf SET and the SCB is described by the coupling coefficient $\kappa=C_c/C_\Sigma$, where C_c is the coupling capacitance between the SET and the SCB and C_Σ is the total capacitance for the SCB. A gate for control of the SCB's electrostatic potential is capacitively coupled to the box with the capacitance C_g [see Fig. 3]. Parameters for the two measured samples are shown in Table I.

The samples are measured at sub-kelvin temperatures in a dilution refrigerator with a base temperature of $\sim$20 mK. All dc lines connected to the sample are heavily filtered with a combination of RCL and powder filters[24,25] to reduce thermal radiation from room temperature. The SCB gate is connected through a 50 Ω matched line with a bandwidth of 50 GHz. This line is used to apply both microwaves and fast pulses[6] to the SCB.

Our setup is equipped with a 3 T magnet that produced a magnetic field parallel to the sample, $B_\parallel$. Since the sample is

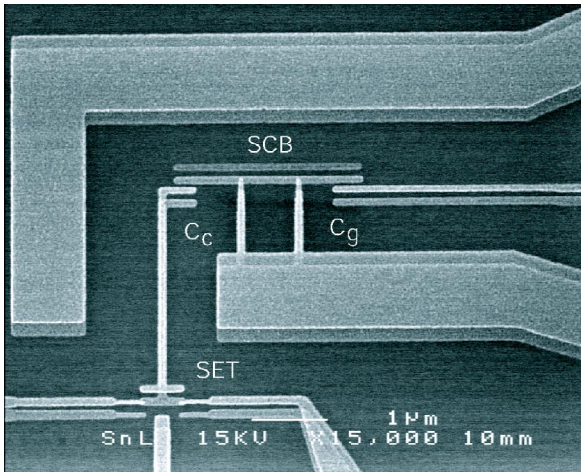

FIG. 3. An electron micrograph of the layout for the integrated SCB and SET.

not perfectly aligned with $B_\parallel$, the magnetic field gives a perpendicular component that threads the SCB loop with 320 mT corresponding to Φ_0. For the measurements of sample A we used a Helmholz coil configuration outside the cryostat which could produce a small field perpendicular to the sample, $B_\perp$, giving less than half a flux quantum in the SQUID loop. For the measurements of sample B, the setup was fitted with a small superconducting coil on the side of the sample holder, which produced a larger perpendicular field, allowing full modulation of E_J.

IV. EXPERIMENTAL RESULTS

By adiabatically ramping the SCB gate voltage V_g and simultaneously measuring the average charge $\langle n \rangle$ of the SCB, we obtain the Coulomb staircase. At zero external parallel magnetic field $B_\parallel$, the Coulomb staircases for both samples had a 1*e* step around the charge degeneracy, which indicates quasiparticle tunnel events onto the SCB. The energy gap $\Delta/k_B \approx 1.9$ K is extracted from the current-voltage characteristics of the SET and should be similar for the SCB. Since for $\Delta \gg k_B T$ we have $\tilde{\Delta} \approx \Delta$ and with $\tilde{\Delta} > E_C - E_J/2$, the SCB should be 2*e* periodic.

However, we find that we can make the SCB completely 2*e* periodic by applying an external magnetic field parallel to the SCB. In sample A, we observed a decrease and eventually an elimination of the 1*e* step with increasing $B_\parallel$. Since an increased magnetic field should lower $\tilde{\Delta}$ and hence increase the 1*e* step in the case of equilibrium, the observed behavior further strengthens the evidence that nonequilibrium quasiparticle processes are involved.

TABLE I. Sample parameters. The table values of E_C and E_J^{max} are measured with microwave spectroscopy. C_g and κ were extracted from the staircase measurements.

Sample	E_C/k_B (K)	E_J^{max}/k_B (K)	C_g (aF)	κ
A	1.25	1.05	14.3	0.033
B	0.43	1.06	39.2	0.012

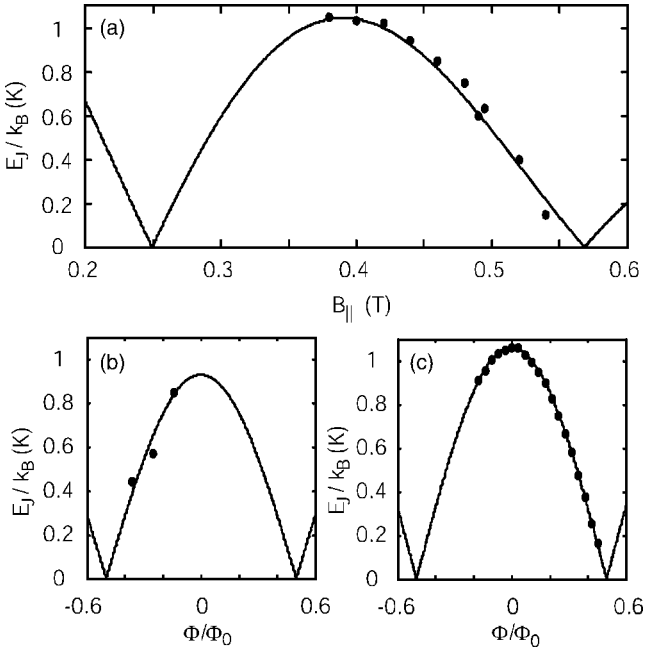

FIG. 4. (a) E_J vs $B_\parallel$ for sample A. The filled circles are measured values of E_J obtained from spectroscopy. They are fitted to Eq. (2) with decreasing $E_J^{\max}(\Delta)$ according to Eq. (3). (b) Measurements of sample A with zero and maximum (positive and negative) flux applied from the Helmholtz coils at $B_\parallel = 460$ mT. They are fitted to Eq. (2), with $E_J^{\max}/k_B = 0.92$ K. (c) E_J vs flux for sample B. The filled circles indicate measurements of E_J from spectroscopy with maximum (positive and negative) flux generated by $B_\perp$. They are fitted to Eq. (2) (solid line).

We suggest that this initial behavior can be explained with magnetic-field-induced "graded gaps." In the fabrication, the SCB island and its connecting leads are made with different thicknesses, where the island is $\approx$25 nm and the leads $\approx$65 nm. The gap in the reservoir is therefore suppressed more than the gap in the island by the applied magnetic field. For a given magnetic field we thus get a smaller gap in the reservoir than in the island, giving graded gaps very similar to the situation in Ref. 17. For even higher $B_\parallel$ the 1*e* step reappears and starts to increase due to the suppression of $\tilde{\Delta}$, and at $B_\parallel = B_{c\parallel}$ the Coulomb staircase is fully 1*e* periodic. Thus for sample A there was a window $370 < B_\parallel < 490$ mT for which the sample was fully 2*e* periodic.

In sample B the 1*e* step was much shorter than for sample A at $B_\parallel = 0$, and it depended strongly on the bias point of the SET (which was not the case for sample A). By biasing at the low end of the double Josephson quasiparticle peak (DJQP),[26] the 1*e* step vanished. However, the sensitivity of the SET was very low at this bias point. With a 300 mT parallel magnetic field applied, both good sensitivity and 2*e* periodicity were achieved for sample B.

In both samples the SCB is formed with a SQUID geometry and thus we can tune E_J with the external magnetic field. E_J depends on the penetrated flux Φ as

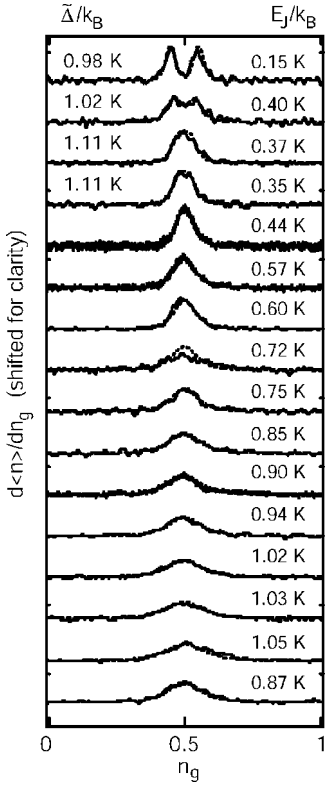

FIG. 5. The derivative of Coulomb staircases (solid lines) that corresponds to $E_J/k_B=0.15$ K up to $E_J/k_B=1.05$ K together with the derivative of the calculated Coulomb staircases obtained from the spectroscopic data (dotted lines). The curves are measured for sample A, and are ordered with increasing $B_\parallel$, from $B_\parallel=370$ mT (bottom) to $B_\parallel=540$ mT (top). At $E_J/k_B=0.35$ K ($B_\parallel=490$ mT) the thermal excitation to the odd charge state broadens the staircase, since $(E_C-E_J/2)\approx\tilde{\Delta}$. For $E_J/k_B=0.15$ K ($B_\parallel=540$ mT) a clear separation into two peaks (the $1e$ step) is visible. Here $(E_C-E_J/2)>\tilde{\Delta}$ and the odd charge state is energetically favorable around the charge degeneracy [see Fig. 1].

$$E_J = E_J^{\max}\left|\cos\left(\frac{\pi\Phi}{\Phi_0}\right)\right| \tag{2}$$

where Φ_0 is the flux quantum, and equal junctions are assumed. E_J^{max} is at low temperature given by[27]

$$E_J^{\max} = \frac{\Delta(B)}{2}\frac{R_Q}{R_N} \tag{3}$$

where $R_Q=h/4e^2$ is the quantum resistance and R_N the junction resistance.

As we tune E_J with $B_\parallel$, we also suppress Δ and thus $\tilde{\Delta}$, and we can extract $\tilde{\Delta}$ from the width of the $1e$ step up to $B_{\parallel c}$.[13,28] By extrapolating $\tilde{\Delta}$ to lower fields where the box is $2e$ periodic we find that $\tilde{\Delta}/k_B$ is suppressed from 1.4 to 1.1 K within the $2e$ periodic window. The suppression of Δ does of course also suppress E_J. By using both magnets we are able to tune E_J/k_B from 0.15 to 1.05 K in sample A, which roughly corresponds to $\Phi_0/2$ [see Figs. 4(a) and 4(b)].

For the measurements of sample B we could use the small coil on the sample holder to apply a flux of a little more than $\Phi_0/2$ through the SCB loop. For sample B we could thus tune E_J/k_B in the range 0.16 to 1.06 K without affecting Δ [see Fig. 4(c)].

Microwave spectroscopy was used to retrieve values of E_C and E_J for each applied magnetic field. With microwaves of frequency ν applied, the SCB is driven between its ground and first excited states, where ν corresponds to the energy separation $\Delta E=E_{n+1}(n_g)-E_n(n_g)$. By continuously measuring $\langle n\rangle$, this driving will turn up as a peak and a dip in $\langle n\rangle$ at n_g^ν where $h\nu=\Delta E$ [Fig. 2(a)]. For sample A, spectroscopy was done at five frequencies and for sample B at 10–20 frequencies for each E_J value. E_J and E_C are extracted by fitting the data to numerically calculated $\Delta E(E_J,E_C,\Delta n_g)$ where $\Delta n_g=|n_g^{dip}-n_g^{peak}|/2$ and six charge states have been included [see Fig. 2(b)].

We can now compare the calculated $\langle n\rangle$ versus n_g staircases[11] evaluated from spectroscopic data with the experimental staircases obtained at the corresponding magnetic fields [Figs. 2(c) and 2(d)]. At high E_J, quasiparticle states and thermal excitations can be neglected, since $\tilde{\Delta}>E_C-E_J/2$ at those fields and the smearing contribution from a

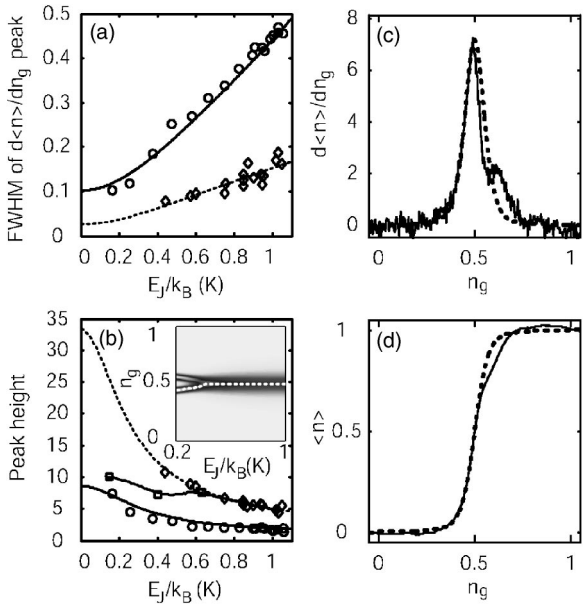

FIG. 6. (a) FWHM of the peak in $d\langle n\rangle/dn_g$ vs E_J, where diamonds are measured values for sample A and circles for sample B. Dotted and solid lines are calculated FWHMS for samples A and B, respectively. (b) Peak height vs E_J, with same legend as in (a). The squares are measurements where the staircase has lost its full $2e$ periodicity. The peak heights are retrieved along the dotted line in the inserted image. The image shows $d\langle n\rangle/dn_g$ vs n_g and E_J where $\tilde{\Delta}$ is a function of E_J. In both (a) and (b), the fact that samples A and B have different E_C's is evident in the slopes and zero crossings of the curves. (c) $d\langle n\rangle/dn_g$ vs n_g for sample B, where the measured trace for $E_J/k_B=0.16$ K is the solid line together with the corresponding calculated trace as the dotted line. The asymmetric behavior is visible as a short shoulder on the right side of the peak. (d) $\langle n\rangle$ vs n_g for the same data as in (c) (same legend). The shoulder feature in (c), is clearly visible as a rounding off of the top edge.

finite T is small. For low E_J, these processes have to be taken into account and we use T as a fitting parameter together with the extrapolated $\tilde{\Delta}(B_\parallel)$.

From the fitted spectroscopy data for sample A we retrieve $E_C/k_B=1.25$ K and E_J ranges from $E_J/k_B=0.42$ K to $E_J/k_B=1.05$ K, within the available 2*e* periodic window. Around $E_J/k_B=0.37$ K, $B_\parallel$ is close to the field where the 1*e* step starts to reappear and $\tilde{\Delta}\approx E_C-E_J/2$, so the staircase is affected by thermal excitation to the odd charge state and a 1*e* step is on the verge of being visible. It should be pointed out that these excitations to the odd charge state are consistent with equilibrium considerations [Figs. 1(a) and 1(b)], and are not due to nonequilibrium quasiparticles.

With $T=75$ mK and the extrapolated $\tilde{\Delta}$ we get a good agreement also for these last points. In Fig. 5, the result is presented as $d\langle n\rangle/dn_g$ for experimental and calculated staircases from $E_J/k_B=0.15$ K to $E_J^{max}/k_B=1.05$ K. Also for sample B we find a good agreement between the calculated and the measured staircases, when E_J is large. The curves are very similar to those shown for sample A in Fig. 5. As E_J/k_B is decreased below 0.47 K a shoulder to the right of the peak emerges in the derivative. Here we used $T=100$ mK as a fitting parameter. This shoulder becomes more evident when E_J is decreased further down to $E_J/k_B=0.16$ K [Figs. 6(c) and 6(d)]. From the spectroscopy we extract $E_C/k_B=0.43$ K and an E_J which ranges from 0.16 K to 1.06 K for sample B.

To get a good measure of how the experimental data fit the calculation we have compared the peak height and peak full width at half maximum (FWHM) of $d\langle n\rangle/dn_g$ for both samples [Figs. 6(a) and 6(b)]. In this representation it shows that the peak heights and FWHMs for sample A agree well both for high E_J and where $\tilde{\Delta}\leqslant E_C-E_J/2$. Peak heights for sample B data are generally somewhat lower than those calculated and when E_J/k_B is decreased below 0.47 K there is a clear discrepancy due to the extra shoulder. This looks similar to the effect of quasiparticle poisoning, but this feature is asymmetric. The reason for this asymmetric behavior is not yet clear, but could be an effect of back action on the SCB due to the SET when biased at the DJQP.[29] Similar asymmetric behavior has been observed by other groups.[7,11]

V. CONCLUSION

In conclusion, we have studied 2*e* periodic Coulomb staircases while tuning E_J in two samples with different E_C, and verified that the shape of the Coulomb staircase corresponds to parameters retrieved from spectroscopy. We have also observed the effect on the Coulomb staircase when it starts to lose its full 2*e* periodicity, due to suppression of $\tilde{\Delta}$, where the shape still depends on E_J. In sample B we observed an asymmetric feature in the staircase at low E_J, which could be an effect of SET back action, but this needs more investigation. We have also shown an alternative way of creating graded gaps in the SCB with the help of a parallel magnetic field.

ACKNOWLEDGMENTS

The samples were made at the MC2 clean room at Chalmers. This work was supported by the Swedish SSF and VR, by the Wallenberg foundation, and by the EU under the IST-SQUBIT program.

*Electronic address: david.gunnarsson@mc2.chalmers.se

[1] Y. Nakamura, Y. Pashkin, and J. Tsai, Nature (London) **398**, 786 (1999).
[2] D. Vion, A. Aassime, A. Cottet, P. Joyez, H. Pothier, C. Urbina, D. Esteve, and M. Devoret, Science **296**, 886 (2002).
[3] Y. Yu, S. Han, X. Chu, S. I. Chu, and Y. Wang, Science **296**, 889 (2002).
[4] I. Chiorescu, Y. Nakamura, C. J. P. M. Harmans, and J. E. Mooij, Science **299**, 1869 (2003).
[5] J. M. Martinis, S. Nam, J. Aumentado, and C. Urbina, Phys. Rev. Lett. **89**, 117901 (2002).
[6] T. Duty, D. Gunnarsson, K. Bladh, and P. Delsing, Phys. Rev. B **69**, 140503(R) (2004).
[7] A. G. Guillaume, J. F. Schneiderman, P. Delsing, H. M. Bozler, and P. M. Echternach, Phys. Rev. B **69**, 132504 (2004).
[8] M. Büttiker, Phys. Rev. B **36**, 3548 (1987).
[9] V. Bouchiat, D. Vion, P. Joyez, D. Esteve, and M. Devoret, Phys. Scr., T **76**, 165 (1997).
[10] Y. Makhlin, G. Schön, and A. Shirman, Nature (London) **398**, 305 (1999).
[11] V. Bouchiat, Ph.D. thesis, Université Paris 6, 1997.
[12] I. Kulik and R. Shekhter, Zh. Eksp. Teor. Fiz. **68**, 623 (1975).
[13] P. Lafarge, P. Joyez, D. Esteve, C. Urbina, and M. H. Devoret, Phys. Rev. Lett. **70**, 994 (1993).
[14] K. K. Likharev and A. B. Zorin, in Proceedings of the 17th International Conference on Low Temperature Physics (Elsevier, Amsterdam, 1984), p. 1153.
[15] P. Lafarge, P. Joyez, D. Esteve, D. Urbina, and M. Devoret, Nature (London) **365**, 422 (1993).
[16] K. W. Lehnert, K. Bladh, L. F. Spietz, D. Gunnarsson, D. I. Schuster, P. Delsing, and R. J. Schoelkopf, Phys. Rev. Lett. **90**, 027002 (2003).
[17] J. Aumentado, M. W. Keller, J. M. Martinis, and M. H. Devoret, Phys. Rev. Lett. **92**, 066802 (2004).
[18] J. Mannik and J. E. Lukens, Phys. Rev. Lett. **92**, 057004 (2004).
[19] K. K. Likharev, IEEE Trans. Magn. **23**, 1142 (1987).
[20] T. A. Fulton and G. J. Dolan, Phys. Rev. Lett. **59**, 109 (1987).
[21] R. J. Schoelkopf, P. Wahlgren, A. A. Kozhevnikov, P. Delsing, and D. E. Prober, Science **280**, 1238 (1999).
[22] A. Aassime, D. Gunnarsson, K. Bladh, R. Schoelkopf, and P. Delsing, Appl. Phys. Lett. **79**, 4031 (2001).
[23] Y. Nakamura, C. D. Chen, and J. S. Tsai, Phys. Rev. Lett. **79**, 2328 (1997).
[24] J. M. Martinis, M. H. Devoret, and J. Clarke, Phys. Rev. B **35**, 4682 (1987).
[25] K. Bladh, D. Gunnarsson, E. Hürfeld, S. Devi, C. Kristoffersson, B. Smålander, S. Pehrson, T. Claeson, and P. Delsing, Rev. Sci. Instrum. **74**, 1323 (2003).

[26] A. Maassen van den Brink, G. Schön, and L. J. Geerligs, Phys. Rev. Lett. **67**, 3030 (1991).
[27] V. Ambegaokar and A. Baratoff, Phys. Rev. Lett. **10**, 486 (1963); **11**, 104(E) (1963).
[28] If $E_J \ll 4E_C$, $\tilde{\Delta}$ can be extracted from the width of the 1*e* step, *S*, through the relation $\tilde{\Delta} = E_C(1-S)$.
[29] A. A. Clerk, S. M. Girvin, A. K. Nguyen, and A. D. Stone, Phys. Rev. Lett. **89**, 176804 (2002).